

# Photothermal reflectance investigation of processed silicon. I. Room-temperature study of the induced damage and of the annealing kinetics of defects in ion-implanted wafers

Constantinos Christofides, I. Alex Vitkin, and Andreas Mandelis

Photoacoustic and Photothermal Sciences Laboratory, Department of Mechanical Engineering and Ontario Laser and Lightwave Research Center, University of Toronto, Toronto, Ontario M5S 1A4, Canada

(Received 3 April 1989; accepted for publication 1 December 1989)

Silicon films damaged by ion implantation have been examined using the photothermal reflectance technique in the thermal wave regime (low-modulation frequencies, large laser beam spot sizes). Data are presented on the sensitivity of this method to the implant dose and to the effects of thermal annealing. It has been shown that the technique provides information about the state of the implanted layer, and is a sensitive probe for monitoring the annihilation of the induced damage as a function of the annealing temperature. A model for the kinetics of damage annihilation has been presented to estimate the activation energy of the *local* annealing recovery mechanism, found to be 0.15 eV. The presence of negative annealing has been detected at about 500 °C, an advantage over the essentially insensitive Hall mobility method.

## I. INTRODUCTION

In recent years, thermal wave techniques have been introduced as a method of characterization of ion-implanted materials.<sup>1-4</sup> In this paper we will show and analyze some results concerning implanted silicon films obtained with the laser-induced photothermal reflectance (PTR) method at ambient temperature. The second paper (Part II)<sup>5</sup> presents, for the first time, a semiquantitative analysis of the variation of the photothermal signal as a function of the measurement temperature.

A useful alternative to high-temperature diffusion is the direct implantation of energetic dopant ions into the semiconductor. Ion implantation, with its capability for great uniformity, impurity profile control, and shallow penetration, is a doping method particularly attractive for the production of shallow *p-n* junctions, which are crucial in modern integrated circuits and solar cell technology. One disadvantage of ion implantation is its generation of defects in the lattice which strongly influence the electronic, optical, and thermal properties of semiconductors. The importance of implanted semiconductor analysis has led to the development of many characterization techniques, such as the following

(i) Electric methods: dc<sup>6</sup> and ac<sup>7</sup> Hall-effect measurements have been employed to characterize implanted semiconductor films. The method of spreading resistance has also been used, allowing measurement of the resistance of the implantation damage layer as a function of depth.<sup>8</sup> These techniques allow one to probe the extent of the created damage, as well as to monitor the annihilation processes of these defects as a function of annealing conditions (i.e., temperature and time). Deep-level transient spectroscopy (DLTS)<sup>9,10</sup> and four-point measurements<sup>11</sup> have also been used for semiconductor characterization. DLTS, with its great sensitivity, has yielded much information about defect states in the gap, even after annealing, while the four

point method gives an evaluation of the average surface resistivity of the material.

(ii) Physicochemical analysis: Rutherford backscattering<sup>12,13</sup> has been used to estimate the proportion of implanted ions residing in interstitial or substitutional sites, and transmission electron microscopy<sup>14</sup> has been employed to study crystallographic defects due to ion implantation.

(iii) Optical methods: An ellipsometric method has been used to study annealing kinetics.<sup>15</sup> Also, infrared absorption experiments have contributed to the knowledge of defect energy levels in the semiconductor gap.<sup>16</sup>

In 1985, Smith *et al.*<sup>1</sup> introduced a new thermal wave technique, photothermal reflectance (PTR), and subsequently applied it to dose monitoring in ion-implanted semiconductors. Although nominally a thermal wave method, PTR has been conventionally and increasingly used as an electron-hole plasma wave probe (MHz-level modulation frequencies and tightly focused, micrometer-sized laser beams) for semiconducting substrate characterization. During the last four years, several workers reported numerous other studies using this technique.<sup>17-22</sup> The technique is particularly useful because of its high spatial resolution, its nondestructive and noncontact nature, and the lack of special sample preparation. However, some difficulties in adequately modeling the physical state of materials damaged by ion implantation still persist, thus impeding the sound understanding and quantitative analysis of the experimental results. Considering the significant amount of information provided by this technique, PTR studies are expected to be very fruitful in elucidating the mechanisms of defect formation and annihilation (due to annealing).

The aim of this paper is to study the dependence of the PTR signal on the implanted dose in the thermal wave regime (kHz-level modulation frequencies and relatively

defocused laser beams) and to monitor the kinetics of thermal annealing. The obtained information can be related to the physical state of the implanted layer, and its evolution under different implantation regimes and different annealing conditions. Comparison with other electrical characterization techniques will also be performed in order to assess PTR's relative sensitivity to the presence of residual defects in implanted layers annealed at different temperatures.

## II. THEORY

The mechanism of the generation of the photothermal signal can be understood in terms of the induced modulation of the refractive index of the illuminated material. In electronically inactive (or low active) materials, the modulated reflectance of the probe beam is primarily based on the temperature dependence of the sample's optical reflectivity. In general, in such solids a small local temperature excursion ( $\Delta T$ ) about average sample temperature,  $T$ , brought about by a light pulse from the heating laser, will cause a corresponding fractional change in the reflectivity of the probe beam:

$$\frac{\Delta R}{R_0} = \frac{1}{R_0} \left( \frac{\partial R}{\partial T} \right) \Delta T, \quad (1)$$

where  $R_0$  is the reflectivity at a reference temperature  $T_0$ , and  $1/R_0(\partial R/\partial T)$  is the temperature coefficient of reflectivity, which is generally a function of the material properties of the sample, its temperature, and the wavelength of the probe beam. In silicon, the introduction of impurities and disorder by the ion implantation process will influence the local temperature rise in several ways: the optical absorption coefficient will increase, increasing the amount of light energy absorbed at the surface; the local thermal and electronic transport coefficients will decrease, allowing less heat to be dissipated from the point of excitation<sup>23</sup>; and the presence of near midgap defect and impurity states will cause an increase in the local nonradiative recombination rate of the photoexcited carriers, thus providing additional heat to the surrounding lattice.<sup>24</sup> Additional heat-generating processes, like nonlinear two-photon absorption, may also be dependent on the degree of local disorder.<sup>25</sup> Thus, the presence of impurities and defects in an ion-implanted layer will cause an increase in the local ac sample temperature and, therefore, in the local thermo-reflectance, over that of the crystalline material. In effect, the "thermal wave" produced in the sample by periodic heating will be strengthened in local amplitude but diminished in spatial extent by the ion implantation process.

In semiconductors, moreover, there is an additional effect brought about by the heating laser whose light energy exceeds the sample's band gap. As pointed out by Opsal *et al.*<sup>26</sup> the electron-hole plasma can also contribute to the photothermal reflectance signal in several ways. There is the dependence of the complex index of refraction on the charge carrier density; there is the photoelectroreflectance effect, whereby the photogenerated plasma may influence the wafer reflectivity by surface band bending; in

addition, the thermalization of the plasma with the lattice, and the subsequent interband recombination will also contribute indirectly to the PTR signal through the above mentioned  $\Delta T$  term. Regardless of the particular mechanism of the plasma effect on reflectivity, we can write for a semiconductor:

$$\frac{\Delta R}{R_0} = \frac{1}{R_0} \left[ \left( \frac{\partial R}{\partial N} \right) \Delta N + \left( \frac{\partial R}{\partial T} \right) \Delta T \right], \quad (2)$$

where  $1/R_0(\partial R/\partial N)$  is the plasma coefficient of reflectivity, and  $\Delta N$  is the local variation in the plasma density brought about by the heating laser. As pointed out by several investigations, the thermal and the plasma wave coefficients of reflectance are often comparable in magnitude and opposite in sign, resulting in a partial net cancellation of the observed signal.<sup>27-29</sup> One way to separate the plasma and the thermal contributions to modulated reflectivity is to vary the product  $\omega\tau$ , where  $\omega = 2\pi f$ , with  $f$  the modulation frequency, and  $\tau$  the lifetime of the photoexcited carriers. Despite a certain ambiguity in assigning a precise value to this relaxation time, it is generally agreed that when  $\omega\tau \ll 1$ , the PTR signal has predominantly thermal origins.<sup>28-30</sup> On the other hand, for  $\omega\tau > 1$ , the plasma effect may become comparable to the thermal effect, or even dominate it. In our experiment, with  $f = 100$  kHz, we expect to detect contributions from both thermal and plasma terms for the nonimplanted crystalline wafer ( $\tau \approx 10^{-6}$  s)<sup>31</sup>; impurities and defects introduced via ion implantation should decrease the plasma contribution since the  $\omega\tau$  term in the damaged surface layer is now much less than unity (carrier lifetimes can be reduced by several orders of magnitude by ion implantation<sup>32</sup>). However, the photogenerated plasma may still contribute indirectly through the thermal term via lattice thermalization and nonradiative-recombination routes.

## III. EXPERIMENT

### A. Silicon samples

The samples which have been used for this study were obtained from two different sources. (100)-oriented,  $n$ -type Si wafers were obtained from Northern Telecom Electronics in Ottawa in 1984. The experimental batch consisted of five pairs of wafers implanted through an oxide layer with  $P^+$  ions with doses between  $1 \times 10^{12}$  and  $1 \times 10^{16}$  ions/cm<sup>2</sup>, at energy of 150 keV. The oxide was then etched away and one member of each pair was thermally annealed at 1100 °C for 15 min in  $N_2$ .

The second experimental batch consisted of (100),  $p$ -type (6  $\Omega$  cm) silicon wafers implanted through a thick oxide layer, at room temperature, with arsenic (dose  $\Phi = 5 \times 10^{14}$  ions/cm<sup>2</sup>; energy  $E = 150$  keV). They were procured from the Microelectronic Center of Grenoble (CIME), France in 1987. Upon removal of the  $SiO_2$  overlayer, some of the samples were thermally annealed isochronally (1 h  $\pm$  20 s) under different temperatures (400, 500, 600 and 800 °C). The withdrawal of the wafers from the furnace to the room-temperature environment was

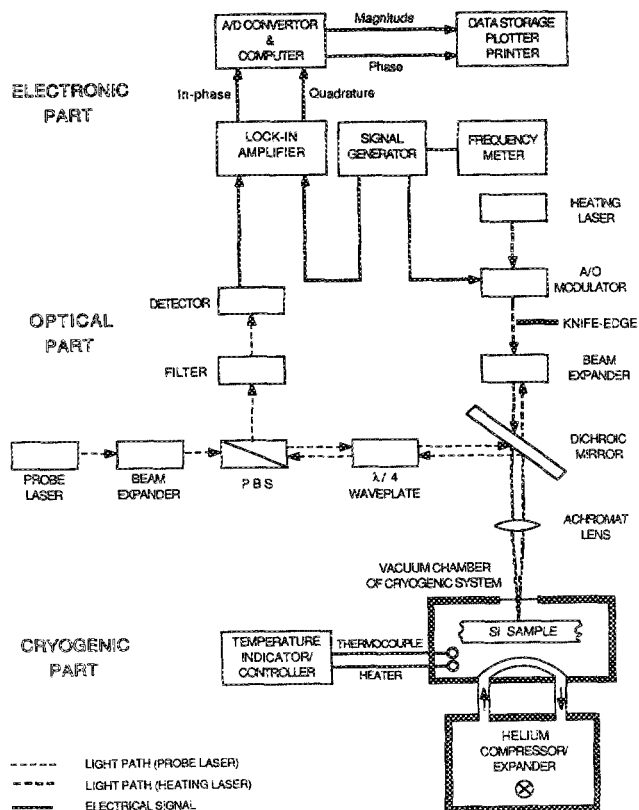


FIG. 1. Experimental setup for the laser-induced photothermal reflectance (PTR) measurements.

controlled automatically. Using spreading-resistance measurements, and the SUPREM simulation program, the junction depths were determined to be approximately  $0.4 \mu\text{m}$ .

### B. Experimental setup

The apparatus used for the PTR studies is shown in Fig. 1; it is similar to the Therma-Probe 150 system, first introduced by Opsal *et al.*<sup>33</sup> The periodic sample heating is obtained with the Ar-ion laser beam (488 nm), acousto-optically modulated at 100 kHz. The beam, of incident power approximately 25 mW, is focussed normally onto the silicon surface to a spot size of about  $30 \mu\text{m}$ . The changes in the reflectivity of a collinear HeNe laser beam (632.8 nm), resulting from the thermal and the plasma waves generated by the heating laser, are measured with a silicon photodiode detector (UDT), filtered by a 632.8-nm bandpass interference filter. In order to reject any signal contributions arising from the thermoelastic deformation of the sample surface, the detector is deliberately under-filled, and is operated in the sum mode. The output of the detector is monitored with a fast lock-in amplifier (EG&G 5202), synchronous with Ar<sup>+</sup> laser modulation of 100 kHz. The in-phase and quadrature components of the signal are stored in the computer for subsequent analysis and display. For a given wafer, about 15 different readings on three different spots of the surface are recorded and then normalized to the signal from the reference crystalline Si sample under identical focusing conditions. The cryogenic

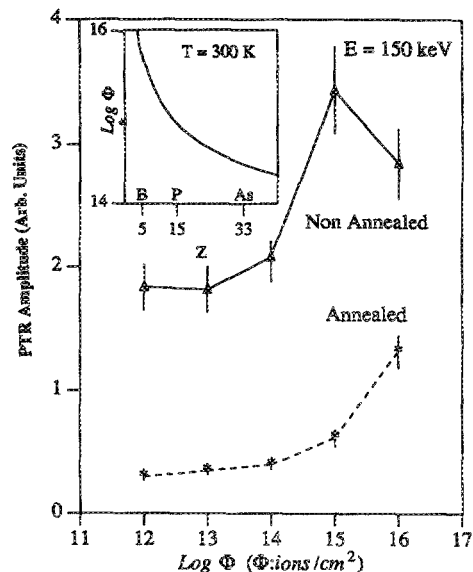


FIG. 2. PTR signal as a function of dose for nonannealed and annealed ( $1100^\circ\text{C}$ , 15 min) P<sup>+</sup>-implanted samples ( $E = 150 \text{ keV}$ , Northern Telecom batch). Inset: critical dose  $\Phi_c$  as a function of atomic number  $Z$  at room temperature.

part of the experimental system (bottom of Fig. 1) is used to study the PTR response as a function of temperature, down to the 20 K range. The results of the temperature studies will be presented and discussed in the companion paper (part II).<sup>5</sup>

### IV. RESULTS AND DISCUSSION

Figure 2 shows the measured photothermal signal as a function of phosphorus dose, over the range  $10^{12}$ – $10^{16}$  ions/cm<sup>2</sup>. The solid curve corresponds to the as-implanted samples, and the dashed one shows the response of the annealed ones. For the nonannealed wafers, we note the increase of PTR signal as a function of dose which becomes more pronounced for high implanted layers. Similar behavior of the photothermal signal has been reported,<sup>17,18</sup> as has the observed saturation which takes place for dose over  $10^{15}$  ions/cm<sup>2</sup>.<sup>34</sup> The observed sensitivity to doping levels is lower than that obtained by the above authors; this has to do with our experimental choice of modulation frequency and laser beam spot sizes. Briefly, with  $f = 100$  kHz, we are primarily sensitive to the changes in the thermal parameters of the damaged layer; it has been recently argued<sup>35</sup> that ion implantation will have a greater effect on the electronic properties of silicon, thus making it advantageous to detect the photogenerated carriers in the plasma-wave regime. These issues will be addressed fully in the companion paper.<sup>5</sup> Presently, we note the increase of the PTR signal with P<sup>+</sup> dose, which is consistent with the higher degree of lattice damage caused by the implantation. In order to better understand the meaning of the observed results, we present the inset of Fig. 2, which shows the variation of the critical dose of amorphization,  $\Phi_c$ , as a function of the atomic number,  $Z$ , of the ions implanted into silicon at room temperature. We note that

$\Phi_c$  increases with decreasing atomic number. According to Christel *et al.*,<sup>36</sup> if the implanted ions displace 10% of the target atoms, the sample can be considered amorphous. If fewer host atoms have been displaced, one speaks of an inhomogeneous layer composed of amorphous clusters within a crystalline matrix. Thus, the implanted layer's amorphization increases with the dose up to the critical dose  $\Phi_c$ ; further implantation will not likely cause any additional structural modification, but will slightly increase the thickness of the damaged layer. This fact can explain the saturation of the PTR signal of the nonannealed wafers at high fluences of Fig. 2, implying that for phosphorus doses of  $10^{15}$  ions/cm<sup>2</sup> or greater, the crystalline-to-inhomogeneous-to-amorphous transition has been completed. Also visible is a slight decrease of the PTR amplitude at the very high dose of  $10^{16}$  P<sup>+</sup>/cm<sup>2</sup>. This implies two possibilities: (i) the decrease is indicative of some physical alteration from the dose  $10^{15}$ – $10^{16}$  ions/cm<sup>2</sup>: this could be due to self-annealing of lattice damage via the heat generated during ion implantation, as suggested by McFarlane and Hess<sup>3</sup>; (ii) the increasing thickness of the amorphous layer is responsible for the signal decrease in this high-dose range, as recently argued by Wurm *et al.*<sup>37</sup> More experimental work is needed to unambiguously resolve this issue.

The photothermal response of samples annealed at 1100 °C for 15 min is somewhat reminiscent of their nonannealed counterparts in that the signal magnitude increases with the ion dose, especially in the high-fluence regime. It seems that this set of annealing conditions is quite effective in returning the layer to a relatively undamaged state for doses less than  $10^{14}$  ions/cm<sup>2</sup> but not for the higher ones. Ishikawa *et al.*,<sup>34</sup> using a similar thermal wave technique, also report the inability of such short time, high-temperature annealing cycle to annihilate the As<sup>+</sup>-induced damage for doses higher than  $10^{15}$  ions/cm<sup>2</sup>. The large post-annealing PTR signal of the sample purported to undergo self-annealing during implantation is consistent with the finding that crystallinity restoration is more difficult to achieve in a heavily damaged but not amorphous material, than in a disordered and amorphous one.<sup>38</sup>

However, for wafers with  $\Phi > 10^{14}$  ions/cm<sup>2</sup>, even a completely recrystallized layer may yield a PTR signal intensity higher than that of c-Si. This is because the dopant atoms (phosphorus in this case), although occupying substitutional sites in the lattice, can significantly increase the impurity scattering processes in the crystal, leading to a greater local temperature rise and thus to a higher PRT signal. Whether our high-dose post-annealing results indicate incomplete recrystallization, or recrystallization with increased impurity scattering, is not clear at present.

Figure 3 shows the photothermal signal as a function of the annealing temperature,  $T_a$ , over the range 400–800 °C; also shown are the signal levels for the nonimplanted and nonannealed samples. Note that annealing at a relatively low temperature of 400 °C causes a noticeable decrease of the PTR signal, implying a significant decrease in local disorder. In fact, according to Boltaks,<sup>39</sup> annealing

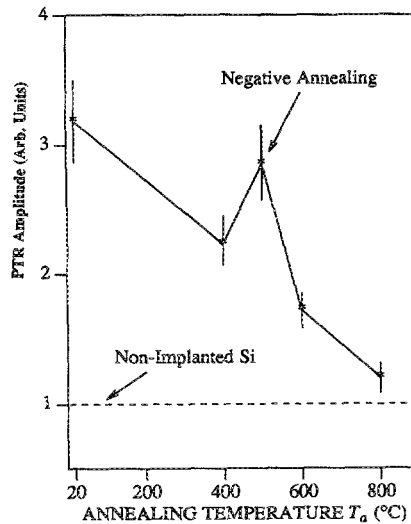


FIG. 3. Variation of the photothermal reflectance signal as a function of annealing temperature for arsenic-implanted silicon wafers. ( $\Phi = 5 \times 10^{14}$  As<sup>+</sup>/cm<sup>2</sup>,  $E = 150$  keV, 1 h annealing time, CIME batch).

at 400 °C is able to annihilate many kinds of point defects such as interstitial vacancy, arsenic vacancy, and divacancies. In Table I,<sup>38–42</sup> we present the various defects induced by ion implantation, the required annealing temperature for their annihilation, and the corresponding activation energies. Also noticeable in the figure is the increase of the PTR signal between 400 and 500 °C, which may be associated with the formation of arsenic complexes. This phenomenon is known as negative or retrograde annealing.<sup>38</sup> It occurs when the concentration of impurities in the damaged host lattice is sufficiently high to promote their migration towards each other as the annealing temperature is raised. Higher annealing temperatures (> 550 °C) are required to dissociate these arsenic defects. As evident from the figure, for high annealing temperatures (> 600 °C), the signal approaches that of the nonimplanted silicon, indicating a high degree of crystallinity restoration. In fact, according to Table I, only line and loop dislocations could survive after an annealing at 800 °C. Although the datum

TABLE I. Defects induced by ion implantation, required temperatures for their annihilation, and the corresponding activation energies.

Type of damage	$T_a$ (°C)	
	$t = 30$ – $60$ min	$E_a$ (eV)
Interstitial vacancy <sup>a,b</sup>	180	0.2–0.5
Arsenic vacancy <sup>a,b</sup>	200	0.8
Divacancy <sup>a,b</sup>	300	1
Layer completely "amorphous" <sup>a</sup>	550–650	2–3
Layer incompletely "amorphous" <sup>a</sup>	700	3–4
Line dislocations <sup>c,d</sup>	800–1000	5–8
Loop dislocations <sup>d,e</sup>	800–1000	5–8

<sup>a</sup>Reference 38.

<sup>b</sup>Reference 39.

<sup>c</sup>Reference 40.

<sup>d</sup>Reference 41.

<sup>e</sup>Reference 42.

at 800 °C is still slightly above the nonimplanted silicon value, we conclude that the dislocation-type defects may not significantly influence the photothermal signal due to the large spatial averaging effected by the 30  $\mu\text{m}$  laser beams. This may be because the dislocations are too few or too small for the beam size averaged signal to "detect" them. Very tightly focused laser beams ( $\approx 1 \mu\text{m}$ ) have been successfully utilized to detect electronically active flaws in silicon wafers.<sup>43</sup>

The kinetics of the annihilation of the damaged layer, as monitored by the PTR method, are consistent with a local annealing process in which the observed photothermal reflectance signal could be described by the relaxation-type relationship<sup>44,46</sup>

$$\Delta R(T_a) = (\Delta R_i - \Delta R_\infty) \exp(-t/\tau_a) + \Delta R_\infty, \quad (3)$$

where  $\Delta R(T_a)$  is the photothermal signal from the annealed wafer at a given temperature,  $\Delta R_i$  is the signal for the as-implanted sample,  $\Delta R_\infty$  is the signal corresponding to nonimplanted wafer (i.e., equivalent to a very high annealing temperature),  $t$  is the annealing duration, and  $\tau_a$  is the relaxation time of the local annealing process. Essentially, we are modeling the recrystallization of the layer by the migration of the implanted As<sup>+</sup> ions (and displaced Si atoms) from interstitial (or other electrically inactive) locations to substitutional/regular lattice sites. To understand the fundamental physics expressed by Eq. (3), we express the annealing behavior of the implanted ions by a first-order reaction-kinetic equation:

$$\frac{dC_i}{dt} = -K_a C_i \quad (4)$$

where  $C_i$  is the concentration of the implanted ions that are initially electrically inactive (e.g., trapped in an interstitial site, bound in a charge complex, localized within a damage cluster, etc.), and  $K_a (= 1/\tau_a)$  is the velocity constant of the annealing reaction in which the implanted ions (and/or displaced Si atoms) migrate to nearby lattice sites and become electrically active.  $K_a$  is energy activated, in accordance with an Arrhenius-type formulation:

$$K_a = K_{a_0} \exp(-E_a/k_B T_a), \quad (5)$$

where  $E_a$  is the activation energy of the local annealing process. The concentration of the electrically active ions,  $C_a$ , depending on the annealing time  $t$  and annealing temperature  $T_a$ , is determined as follows:

$$C_a(t, T_a) = C_a(0,0) + C_i(0,0) - C_i(t, T_a), \quad (6a)$$

$$C_{a,\text{max}} = C_a(0,0) + C_i(0,0). \quad (6b)$$

$C_a(0,0)$  is the portion of ions which are already electrically active without annealing (this depends on the implantation temperature and dose);  $C_i(0,0)$  is the quantity of ions which are not active without annealing;  $C_i(t, T_a)$  is the instantaneous density of inactive ions, which decrease exponentially with time and annealing temperature, as suggested by Eqs. (4) and (5); and  $C_{i,\text{max}}$  is the maximum concentration of electrically active ions, which should occur in the limit of long times and high temperatures. By

integrating Eq. (4) and substituting the solution into Eqs. (6), one obtains for a first-order process:

$$\frac{C_{a,\text{max}} - C_a(0)}{C_{a,\text{max}} - C_a(T_a)} = \exp(K_a t). \quad (7)$$

We can now replace the electrically active ion concentrations  $C_a$ 's with the photothermally measured quantities  $\Delta R$ 's since the PTR signal monitors the damaged layer restoration and is thus an indicator of the electrical activation of impurities (this may be justified with other experimental quantities that depend on the state of the lattice and the transport properties, such as thermal and electrical conductivities, electrical mobility, spreading resistance, and so on). This substitution gives

$$\frac{\Delta R_i - \Delta R_\infty}{\Delta R(T_a) - \Delta R_\infty} = \exp(K_a t), \quad (8)$$

which is equivalent to our initial relation, Eq. (3). Defining the left-hand member of Eq. (8) as the reduced photothermal signal  $Q$ , and combining with Eq. (5), we finally obtain

$$\ln(Q) = (K_{a_0} t) \exp(-E_a/k_B T_a). \quad (9)$$

Thus, plotting the double logarithm of  $Q$  vs  $1/T_a$  should yield a straight line of slope  $-E_a/k_B$ . To construct this plot we must ignore the experimental point in the negative annealing regime, because this presumed "global amorphization" process of complex As defect formation is not governed by Eq. (8). Performing the appropriate calculations, we obtain the plot shown in Fig. 4(a), where the region in the 450–550 °C range is indicated with a dashed line. The measurement of the slope yields  $E_a \approx 0.15$  eV. The small value of  $E_a$  is most likely attributable to a local migration of point defects (see Table I), and is consistent with the proposed mechanism of local migration of arsenic and silicon atoms to the regular lattice sites. It also differs from the usual value (2–3 eV) which is characteristic of a mechanism involving propagation of the recrystallization front from the substrate towards the surface.<sup>47</sup>

As previously mentioned, the parameter  $Q$  of Eq. (9) can represent various quantities that monitor the damaged layer restoration. In Fig. 4(b), we present a similar double-logarithmic plot using Hall mobility measurements of arsenic implanted  $n$ -type silicon taken from Ref. 48. Note that the activation energies of the annealing process are essentially in the range of annihilation of point defect (vacancy)-related damage, Table I. As seen from Table I,  $E_a$  values less than 1 eV do indeed correspond to the local migration of point defects, in agreement with the proposed model. The actual differences in the values of  $E_a$  may be due to the different nature of signal generation between the PTR and the Hall-effect methods: the latter characterization technique is primarily sensitive to electrical transport processes in the layer, whereas our study is mostly influenced by the thermal effects (at 100 kHz modulation frequency with relatively unfocused beams). This difference in the origin of the measured signals may also explain the

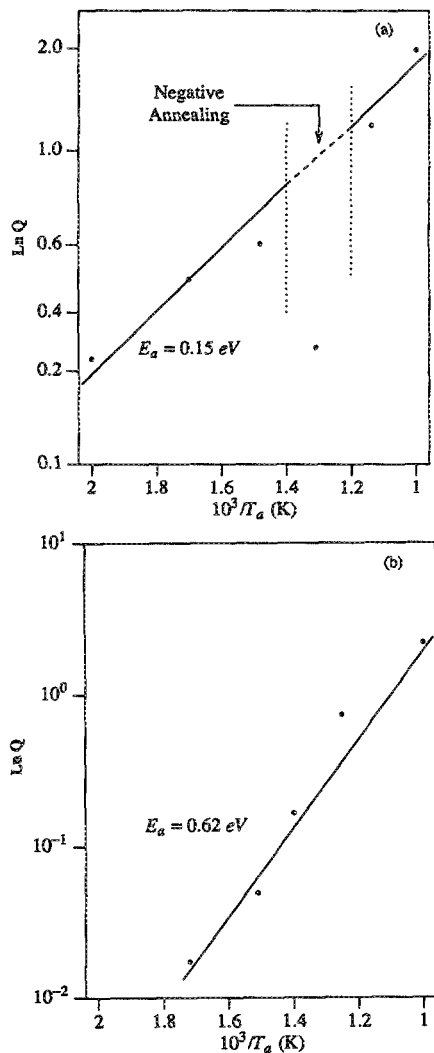


FIG. 4. (a) Determination of the activation energy of the local annealing process using PTR results. The region corresponding to the negative annealing regime is indicated with a dashed line. (b) Similar analysis using Hall mobility measurements ( $\Phi = 8 \times 10^{14} \text{ As}^+/\text{cm}^2$ ,  $E = 120 \text{ keV}$ , 1 h annealing time). Reproduced by permission from Ref. 48.

inability of the Hall mobility measurements to detect the negative annealing regime, which was also detectable by the ac conductivity characteristic frequency (ac van der Pauw) technique.<sup>48</sup> Overall, it appears that the PTR technique, coupled with the data analysis approach summarized in Eq. (9), is indeed sensitive to the local rearrangement of the defects such as the migration of interstitial atoms.

## V. CONCLUSIONS

In this paper, we have used photothermal reflectance experiments to study the influence of implantation of silicon by arsenic and phosphorus impurities on the thermal-wave-induced signal, as complementary to the more conventional studies with electron-hole plasma-wave-induced signals. The crystallinity restoration effectiveness of short-time, high-temperature anneal (1100 °C, 15 min) in phosphorus-implanted layers has been examined. In addition,

we have reported the influence of thermal annealing at different temperatures in order to study the annihilation of defects induced by arsenic ion implantation. Qualitative discussions relating the magnitude of the PTR signal to the local conditions of the layer (presence and types of defects, inhomogeneous/amorphous transition, etc.) have also been performed, as well as a quantitative analysis of the annealing kinetics of defects.

The main results of our study can be summarized as follows:

(1) The strong influence of the implant dose on the PTR thermal wave signal which points out the degree of the induced disorder in the damaged layer; comparison with studies performed in the plasma wave regime suggests that ion implantation has a larger effect on electronic properties than on the thermal properties of the system.

(2) The strong increase of the PTR signal around the critical dose and its subsequent saturation, which indicates the crystalline-to-inhomogeneous-to-amorphous transformation of the implanted layer.

(3) The PTR sensitivity to residual damage after annealing and its ability to detect the anomalous (“negative”) annealing temperature regime, which cannot be detected by conventional Hall mobility measurements.

(4) The large effect of the annealing temperature on the PTR thermal wave signal of the implanted layers. Annealing times longer than 15 min appear to be necessary to recrystallize heavily damaged layers, even at  $T_a = 1100 \text{ °C}$ . The activation energy of the local annealing recovery mechanism in arsenic-damaged silicon has been found to be  $E \approx 0.15 \text{ eV}$ .

(5) It seems that the 100 kHz PTR thermal wave signal (induced by a laser beam of 30  $\mu\text{m}$  spot size) is not very sensitive to the presence of dislocation-type defects.

- <sup>1</sup>W. L. Smith, A. Rosencwaig, and D. Willenborg, *Appl. Phys. Lett.* **47**, 584 (1985).
- <sup>2</sup>D. Guidotti and H. M. van Driel, *Appl. Phys. Lett.* **47**, 1336 (1985).
- <sup>3</sup>R. A. McFarlane and L. D. Hess, *Appl. Phys. Lett.* **36**, 137 (1981).
- <sup>4</sup>J. F. Zucco and A. Mandelis, *Ultrason. Ferroelectr. Freq. Control* **UFFC-35**, 5 (1988).
- <sup>5</sup>I. A. Vitkin, C. Christofides, and A. Mandelis, *J. Appl. Phys.* **67**, 2822 (1990).
- <sup>6</sup>L. J. Van der Pauw, *Philips Res. Rep.* **13**, 1 (1958).
- <sup>7</sup>H. Jaouen, G. Ghibaud, and C. Christofides, *J. Appl. Phys.* **60**, 1699 (1986).
- <sup>8</sup>J. R. Ehrstein, in *Nondestructive Evaluation of Semiconductor Materials*, edited by J. N. Zemel (Plenum, New York, 1979), Chap. 1.
- <sup>9</sup>N. M. Johnson, J. L. Regolini, and D. J. Bartelink, *Appl. Phys. Lett.* **36**, 425 (1980).
- <sup>10</sup>L. C. Kimmerling and J. L. Benton, *Laser and Electron Beam Processing of Materials*, edited by C. W. White and P. S. Peercy (Academic, New York, 1980), p. 385.
- <sup>11</sup>D. S. Perloff, *Solid State Electron.* **20**, 681 (1977).
- <sup>12</sup>S. T. Picraux, *Defects in Semiconductors*, edited by J. Narayan and T. Y. Tan (North-Holland, New York, 1981), Vol. 2, p. 135.
- <sup>13</sup>W. M. Paulson and J. R. Wilson, *Defects in Semiconductors*, edited by S. Mahajan and J. W. Corbett (North-Holland, New York, 1983), Vol. 14, p. 523.
- <sup>14</sup>W. Krakow, T. Y. Tan, and H. Foell, *Defects in Semiconductors*, edited by J. Narayan and T. Y. Tan (North-Holland, New York, 1981), Vol. 2, p. 185.
- <sup>15</sup>H. J. Stein, J. A. Knapp, and P. S. Peercy, *Laser and Electron Beam Interactions with Solids*, edited by B. R. Appleton and G. K. Celler (Elsevier, Amsterdam, 1982), p. 319.

- <sup>16</sup>J. Luo, H. J. McMarr, and K. Vedam, *Defects in Semiconductors*, edited by S. Mahajan and J. W. Corbett (North-Holland, New York, 1983), Vol. 14, p. 529.
- <sup>17</sup>W. L. Smith, A. Rosencwaig, D. L. Willenborg, J. Opsal, and M. W. Taylor, *Solid State Technol.* **29**, 85 (1986).
- <sup>18</sup>B. J. Kirby, L. A. Larson, and R. Liang, *Nucl. Instrum. Methods B* **21**, 550 (1987).
- <sup>19</sup>J. Schuur, C. Waters, J. Maneval, N. Tripsis, A. Rosencwaig, M. Taylor, W. L. Smith, L. Golding, and J. Opsal, *Nucl. Instrum. Methods B* **21**, 554 (1987).
- <sup>20</sup>M. A. Wendman and W. L. Smith, *Nucl. Instrum. Methods B* **21**, 559 (1987).
- <sup>21</sup>N. Uchitomi, H. Mikami, N. Toyoda, and R. Nii, *Appl. Phys. Lett.* **52**, 30 (1988).
- <sup>22</sup>W. L. Smith, M. W. Taylor, and J. Schuur, *SPIE Proc.* **530**, 201 (1985).
- <sup>23</sup>J. Zammit, M. Marinelli, F. Scudieri, and S. Martellucci, *Appl. Phys. Lett.* **50**, 830 (1987).
- <sup>24</sup>P. Kireev, *Physics of Semiconductors* (Mir, Moscow, 1975), Chap. 6.
- <sup>25</sup>I. W. Wylie and E. P. C. Lai, *Chemtronics* **1**, 69 (1986).
- <sup>26</sup>J. Opsal, M. W. Taylor, W. L. Smith, and A. Rosencwaig, *J. Appl. Phys.* **61**, 240 (1987).
- <sup>27</sup>J. Opsal and A. Rosencwaig, *Appl. Phys. Lett.* **47**, 498 (1985).
- <sup>28</sup>F. A. McDonald, D. Guidotti, and T. M. DeGiudice, IBM Internal Report No. 54561 (April 1986).
- <sup>29</sup>D. Guidotti and H. M. van Driel, *Appl. Phys. Lett.* **49**, 301 (1986).
- <sup>30</sup>A. Skumanich, D. Fournier, A. C. Boccara, and N. M. Amer, *Appl. Phys. Lett.* **47**, 402 (1985).
- <sup>31</sup>B. G. Streetman, *Solid State Electronic Devices*, 2nd ed. (Prentice-Hall, New York, 1980), Chap. 4.
- <sup>32</sup>A. Mogro-Campero and R. P. Love, *Thirteenth International Conference On Defects in Semiconductors*, edited by L. C. Kimerling and J. M. Parsey, Jr. (Metallurgical Society, Pennsylvania, 1985), p. 565.
- <sup>33</sup>J. Opsal, A. Rosencwaig, and D. Willenborg, *Appl. Opt.* **22**, 3169 (1983).
- <sup>34</sup>K. Ishikawa, M. Yoshida, and M. Inoue, *Jpn. J. Appl. Phys.* **26**, L1089 (1987).
- <sup>35</sup>J. Opsal, Technical Digest, Sixth International Conference on Photoacoustic and Photothermal Phenomena, Baltimore, MD, 1989, paper WPM2; p. 20; and private communication.
- <sup>36</sup>L. A. Christel, J. F. Gibbons, and T. W. Sigmon, *J. Appl. Phys.* **52**, 7143 (1981).
- <sup>37</sup>S. Wurm, P. Alpern, D. Savignac, and R. Kakoschke, *Appl. Phys. A* **47**, 147 (1988).
- <sup>38</sup>J. F. Gibbons, *Proc. IEEE* **60**, 1062 (1972).
- <sup>39</sup>B. Boltaks, *Diffusion in Semiconductors* (Mir, Moscow, 1977), Chaps. 2 and 3.
- <sup>40</sup>T. Tamura, *Appl. Phys. Lett.* **23**, 651 (1973).
- <sup>41</sup>C. Kittel, *Introduction to Solid State Physics*, 5th ed. (Wiley, New York, 1983), Chap. 17, 18.
- <sup>42</sup>R. Klages, J. Matthai, M. Voelskow, and G. A. Kachurn, *Phys. Status Solidi A* **66**, 261 (1981).
- <sup>43</sup>G. E. Carver and J. D. Michalski, *SPIE Proc.* **794**, 152 (1987).
- <sup>44</sup>C. S. Fuller, *Semiconductors*, edited by N. B. Hannay (Reinhold, New York, 1959), Chap. 5.
- <sup>45</sup>C. Christofides, G. Ghibauda, and H. Jaouen, *Rev. Phys. Appl.* **22**, 407 (1987).
- <sup>46</sup>H. Ryssel and I. Ruge, *Ion Implantation* (Wiley, New York, 1986), Chap. 3.
- <sup>47</sup>S. Kokorowski, G. Olson, and L. Hess, *J. Appl. Phys.* **53**, 921 (1982).
- <sup>48</sup>C. Christofides, G. Ghibauda, and H. Jaouen, *J. Appl. Phys.* **65**, 4840 (1989).